Microbiology and Immunology

Microbiol Immunol 2011; **55**: 673–682
doi:10.1111/j.1348-0421.2011.00368.x

ORIGINAL ARTICLE

Modulation of poly-*N*-acetylglucosamine accumulation within mature *Staphylococcus epidermidis* biofilms grown in excess glucose

Filipe Cerca[1,2], Ângela França[3], Rodrigo Guimarães[1], Mariana Hinzmann[1], Nuno Cerca[3], Alexandre Lobo da Cunha[1], Joana Azeredo[3], and Manuel Vilanova[1,2]

[1]Institute of Biomedical Sciences Abel Salazar, Oporto University, Largo do Professor Abel Salazar 2, 4099–003, Oporto, Portugal; [2]Institute for Molecular and Cellular Biology, Rua do Campo Alegre 83, Oporto, Portugal; [3]Center of Biological Engineering, Institute of Biotechnology and Bioengineering, Campus de Gualtar, Minho, Braga, Portugal

ABSTRACT

PNAG is a major component of *Staphylococcus epidermidis* biofilms involved in intercellular adhesion as well as in the interaction of the biofilm with components of the host immune response. Synthesis of PNAG has been found to be regulated by several environmental factors. In the present study, the effect of glucose metabolism-dependent culture medium acidification in PNAG accumulation was evaluated. Established *S. epidermidis* biofilms were allowed to grow in excess glucose with or without maintained pH conditions. PNAG accumulation in these biofilms was determined by flow cytometry and fluorescence microscopy using wheat germ agglutinin as a fluorescent probe. Biofilms grown in maintained pH conditions presented significantly higher amounts of this polymer as well as higher *icaA* expression than biofilms grown in acidic pH conditions. Moreover, PNAG accumulation in biofilms grown in non-maintained pH conditions occurred in association with cell death. Overall, we show that glucose metabolism by decreasing the culture pH affects biofilm physiology in respect to PNAG production and cell death. The reported *in vitro* modulation of PNAG accumulation within *S. epidermidis* biofilms further highlights the role of environment on determining the biofilm physiological state.

Key words biofilms, *S. epidermidis*, poly-*N*-acetylglucosamine, cell death.

The coagulase-negative *Staphylococcus epidermidis* is among the leading causes of nosocomial infections (1). These infections usually originate in biofilms established on the surface of indwelling medical devices (2). The physiological properties of biofilms, such as the presence of large amounts of dormant bacteria (3, 4) or the presence of an embedding extracellular matrix (5) make these infections very difficult to treat and eradicate, often leading to the surgical removal of the implanted medical device (6).

S. epidermidis biofilm formation involves the initial attachment of bacteria to a surface mediated by different surface proteins known as MSCRAMMs (5). Subsequent to the initial adhesion phase, a key component in the development of the biofilm is the production of PNAG, the major intercellular adhesin of *S. epidermidis* biofilms (7). In addition to mediate biofilm cohesion, PNAG is also considered a virulence factor of *S. epidermidis* biofilms. This has been demonstrated by independent studies showing that *S. epidermidis* mutants lacking enzymes involved in

Correspondence
Manuel Vilanova, Instituto de Ciências Biomédicas de Abel Salazar, Largo do Professor Abel Salazar 2, 4099-003, Porto, Portugal. Tel: 351-222062250; fax: 351-222062232; email: vilanova@icbas.up.pt

Received 24 February 2011; revised 17 June 2011; accepted 29 June 2011.

List of Abbreviations: CFU, colony forming unit; DAPI, 4′,6-diamidino-2-phenylindole; FITC, fluorescein isothiocyanate; FSC-H, forward scatter; HPO_4^{2-}, hydrogen phosphate; HSD, honestly significant differences; MSCRAMMs, microbial surface components recognizing adhesive matrix molecules; PBS, phosphate-buffered saline; PI, propidium iodide; PNAG, poly-*N*-acetylglucosamine; SD, standard deviation; SSC-H, side scatter; SYBR, SYBR green I; TSA, tryptic soy agar; TSB, tryptic soy broth; WGA, wheat germ agglutinin.

PNAG synthesis had attenuated virulence (8,9). PNAG has been also shown to be an important immunogenic component with the ability to regulate pro-inflammatory cytokine production (10).

PNAG synthesis is dependent on a set of enzymes encoded by genes within the intercellular adhesin (*icaADBC*) locus (11). Expression of these genes has been shown to depend on diverse environmental conditions (12, 13, 14, 15), including high concentrations of glucose (16). It was proposed that *S. epidermidis* may perceive external environmental changes through alterations in the bacterial metabolic status (17). This would in turn mediate genetic regulation of the *icaADBC* operon resulting in the attenuation or augmentation of PNAG production (18).

Glucose has a key role in biofilm physiology. In oral biofilms, glucose metabolism leads to accumulation of acidic end-products responsible for decreasing the environmental pH, which contributes to caries development (19). This also affects the bacterial phenotype as cells within biofilms adapt to the transient glucose-dependent low culture pH by developing an acid tolerance response (20). Glucose is also the most common osmotic agent from dialysis fluid and, therefore, is the major nutrient supporting bacterial growth and biofilm establishment into peritoneal dialysis catheters (21). These biofilms have been described as the principal cause of recurrent peritonitis (22).

In the present study, we evaluated the effect of culture medium acidification due to glucose metabolism in PNAG accumulation within *S. epidermidis* biofilms. Established biofilms were allowed to grow in excess glucose with or without maintained pH conditions. PNAG accumulation and *icaA* expression was evaluated in these biofilms. Our results show that *in vitro* culture conditions, namely glucose-dependent acidic pH, strongly influences PNAG accumulation within *S. epidermidis* biofilms.

MATERIALS AND METHODS

S. *epidermidis* bacterial cultures

In this study, the previous characterized biofilm forming strains were used: 9142, PE9, M187, JI6, IE86 and IE214 (23). TSB (Merck, Darmstadt, Germany) and TSA (Merck) were prepared according to the manufacturer's instructions. *S. epidermidis* grown on TSA plates was used to inoculate 50 mL of TSB subsequently incubated at 37°C in a shaker rotator at 80 rpm for 18 hr. Cells were then harvested by centrifugation (10 min at 10500 *g* at 4°C), ressuspended in PBS and the optical density at 640 nm was adjusted to 0.250 (±0.05). To stimulate biofilm growth, 10μL of the bacterial suspension was transferred to a well of a polystyrene plate (Nunc, Roskilde, Denmark) containing 1 mL of TSB supplemented with 0.3% of glucose (w/v) (Merck) and incubated in a shaker rotator at 37°C and 80 rpm for 24 hr, so a mature biofilm could be established (16, 24). These established biofilms were used as a starting point to evaluate the effect of excess glucose and culture medium acidification in PNAG accumulation within *S. epidermidis* biofilms. For this purpose, the growth medium was removed, and biofilms were allowed to grow an additional 24 hr in TSB supplemented with 1% of glucose (w/v) (TSB 1%G) (Merck) or TSB 1%G supplemented with 100 mM disodium hydrogen phosphate (Merck) (TSB 1%G + HPO_4^{2-}).

For evaluating the effect of vancomycin in planktonic bacteria, 100 μL of the bacterial suspension were transferred to a polystyrene tube containing 400 μL of TSB or TSB with vancomycin (40 μg/mL) (Sigma, St Louis, MO, USA), previously shown to be an effective antibiotic against planktonic *S. epidermidis* cells (25), and incubated in a shaker rotator at 37°C and 80 rpm for 2 hr.

Cell preparation and staining

S. epidermidis biofilms were carefully washed twice with 1 mL of PBS to remove planktonic cells in the culture supernatant. The biofilm was then mechanically disrupted in 1 mL of PBS using a sterile embolus from a 1-mL syringe. Biofilm-grown bacteria were transferred to a polystyrene tube and gently sonicated on ice, at 18 W for 10 s, with the sonicator tip placed at the air/liquid interface (Branson model W 185 D ultrasonic cell disrupter; Heat Systems-Ultrasonics, Plainview, NY, USA). This treatment did not reduce cell culturability, as determined by CFU counting, or affect cell membrane permeability, as determined by PI incorporation (Supplementary Fig. 1). Sonication eliminated bacterial aggregates as determined by flow cytometry assessing Forward (size) and Side (internal complexity) scatter profiles of the bacterial samples before and after sonication (Supplementary Fig. 1). After vortexing, 30 μL of the cell suspensions were transferred to 270 μL of PBS containing SYBR green I (SYBR) (Invitrogen, Carlsbad, CA, USA) (1:5000, commercial stock) and different concentrations (5, 1, 0.5, 0.1 and 0.05 μg/mL) of PI (Sigma).

For evaluating surface *N*-acetylglucosamine in bacteria, 30 μL of the biofilm cell suspensions were transferred to 270 μL of PBS containing FITC-conjugated wheat germ agglutinin (FITC-WGA) (Sigma) (10 μg/mL) (26) and PI (Sigma) (5 μg/mL). Cells were incubated for 10 min at 4°C.

For evaluating the SYBR/PI staining profile of planktonic bacteria upon growth in the presence of vancomycin, 30 μL of the planktonic growth was transferred, at each hour, to 270 μL of PBS containing SYBR (1:5000,

commercial stock), PI (5 μg/mL) and 3 μL of fluorescent counting beads (Invitrogen).

Flow cytometry

The bacterial fluorescence analysis was carried out using a FACScan (Becton-Dickinson, San Jose, CA, USA) containing a low-power aircooled 15 mW blue (488 nm) argon laser. Data was acquired using the CellQuest software (Becton-Dickinson) and analyzed using the Flowjo 7.2.5 software (Tree Star, Ashland, OR, USA). Multiparametric analyses were performed on both scattering signals (FSC, SSC) and FL1/FL3 channels. SYBR fluorescence was detected on FL1 channel (BP530/30) while PI fluorescence was detected on FL3 channel (LP650). For all detected parameters, amplification was carried out using logarithmical scales.

Real time PCR

Total cellular RNA was prepared using the FastRNA Pro Blue Kit (MP Biomedicals, Solon, OH, USA) as described previously (27). Contaminating DNA was removed by treatment with DNaseI (Fermentas, Ontario, Canada) for 30 min at 37°C. The enzyme was heat-inactivated at 65°C for 10 min in the presence of EDTA. RNA was quantified using a Nanodrop (Thermo Scientific, Waltham, MA, USA) and stored at –80°C. The primers used to amplify *icaA* and 16S rRNA were designed using Primer3 (28) based on *S. epidermidis* RP62A genome: *icaA*_FW (GACCTCGAAGTCATAGAGG), *icaA*_REV (TTGCATATTCAATGGTCTGT); 16S_FW (AATCTTGACATCCTCTGACC) and 16S_REV (AGAGTGCCCAACTTAATGAT), respectively. RNA samples were reverse transcribed in the presence of *icaA*_REV, and 16S_REV and M-uLV Reverse Transcriptase (Fermentas). Control reactions lacked reverse transcriptase enzyme. For amplifying *icaA*, 1:40 dilutions of cDNA and no-RT controls were used and for 16S rRNA 1:800 dilutions were used. Realtime RT-PCR reactions contained 2 μL diluted cDNA or no-RT control, 10 pmol of each primer, 6 μL nuclease free deionized H2O, and 10 μL SsoFastTM Evagreen supermix (Bio-Rad, Hercules, CA, USA). Real time RT-PCR (Bio-rad CFX 96) was performed under the following conditions: 95°C for 30 s, 39 cycles of 95°C for 5 s and finally 60°C for 20 s. To monitor the specificity, final qRT-PCR products were analyzed by melting curves.

Glucose, phosphate and pH measurements

Established 24 hr-grown biofilms were allowed to grow for an additional 24 hr as described. At 3-hr intervals, supernatant aliquots were removed, centrifuged at 20 800 *g* for 5 min at 4°C and stored at –20 °C until use. Glucose and phosphate concentration were determined using commercially available quantification kits (R-Biopharm for glucose, Innoprot for phosphate) according to the manufacturer's instructions. The supernatant pH was determined with a pH meter (WTW pH 330).

Fluorescence microscopy

Intact *S. epidermidis* biofilms grown for 48 hr as described were washed twice with 1 mL of PBS. The biofilms were then stained with DAPI (Sigma) (5 μg/mL), FITC-WGA (10 μg/mL) and PI (5 μg/mL) for 5 min at 4°C. Fluorescence was analyzed in an AxioImager Z1 (Carl Zeiss, Göttingen, Germany) using Axiovision 4.6 software.

Statistical analysis

Independent unpaired data were analyzed with Student's *t*-test; multigroup comparisons were analyzed using the ANOVA Tukey's HSD post-hoc test analyzed with the SPSS software (IBM, Chicago, IL, USA). Figure legends indicate the method used for data presentation. A *P*-value less than 0.05 was considered significant.

RESULTS

Flow cytometric identification of distinct bacterial populations in *Staphylococcus epidermidis* biofilms

In order to characterize *S. epidermidis* 9142 bacteria within biofilms grown for 48 hr in TSB 1%G, these were mechanically disrupted and the resulting cell suspensions were analyzed by flow cytometry. As shown in Figure 1a, forward (FSC-H) and side (SSC-H) scattering signals allowed bacteria to be discriminated from the instrument background signal. To evaluate the proportions of dead bacteria in the biofilm cells, these were first stained with PI, a stain that is membrane impermeant entering only in membrane-damaged cells. As shown in Figure 1b, besides PI^- cells, two PI^+ bacterial populations could be discriminated according to their respective SSC-H values (SSC^{high} and SSC^{low}). In order to better characterize the detected bacterial populations, cells were stained with SYBR and PI. SYBR, in contrast to PI, is membrane permeant entering in both live and dead cells. As shown in Figure 1c, staining biofilm cells with SYBR and PI allowed a better discrimination of the three detected bacterial populations. These populations were defined as $SYBR^+PI^-$ (R1), $SYBR^+PI^+$ (R2) and $SYBR^-PI^+$ (R3). The R1 population was the only PI^- population thus containing live cells only. The R3 population presented the same SYBR/PI staining profile of acetone-fixed bacteria (Fig. 1d) and, therefore,

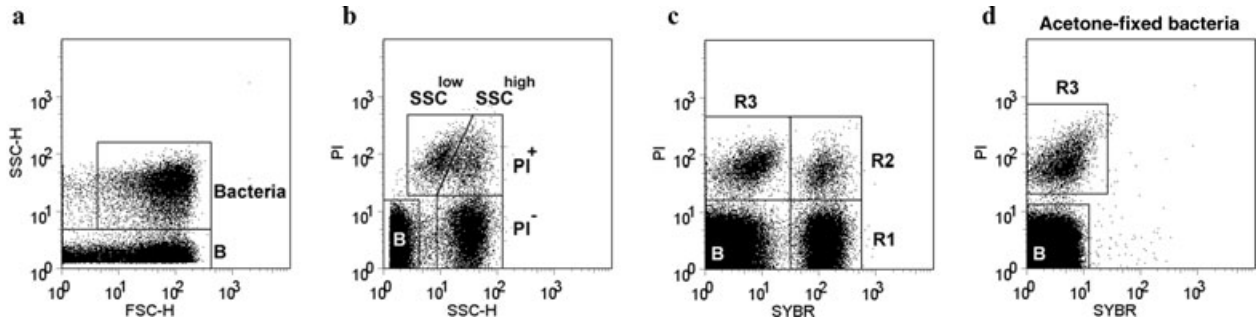

Fig. 1. Flow cytometric analysis of *S. epidermidis* bacteria obtained from 48-hr-grown biofilms. (a) Representative dot plot (FSC-H vs SSC-H signals) showing the discrimination of *S. epidermidis* cells (Bacteria) from the instrument background signal (B). (b) Representative dot plot (SSC-H vs FL3 channel) showing *S. epidermidis* cells stained with PI (5 μg/mL). Regions delimiting bacteria that incorporated PI (PI^+) or impermeable to PI (PI^-) are shown. The SSC-H signal intensity of PI^+ subpopulations (SSC^{high} and SSC^{low}) is also shown. (c) Representative dot plot (FL1 vs FL3 channel) showing *S. epidermidis* cells stained with PI (5 μg/mL) and SYBR green I (SYBR) (1:5000, commercial stock). Three bacterial populations respectively designated R1, R2 and R3 could be discriminated from the instrument background signal (B). (d) Representative dot plot (FL1 vs FL3 channel) showing the SYBR/PI staining profile of acetone-fixed *S. epidermidis* cells stained with PI and SYBR.

contained dead cells only. The R2 population presented staining characteristics of both live ($SYBR^+$) and dead (PI^+) cells. The instrument background (B) was determined using a sample without bacteria.

Effect of PI concentration on the SYBR/PI double staining profile

The $SYBR^+PI^+$ (R2) bacteria remained undefined in respect to their live/dead state. A previous report proposed that the double positive stain in cells could be a consequence of low PI staining concentrations that, in turn, would allow the other dye to compete with PI for the same DNA binding sites (29). We have thus evaluated the SYBR/PI staining profile in biofilm-grown *S. epidermidis* bacteria that were stained with decreasing concentrations of PI (5, 1, 0.5, 0.1 and 0.05 μg/mL) and a fixed concentration of SYBR. As shown in Figure 2, R2 and R3-gated bacteria presented increasing SYBR mean intensity fluorescence (MFI) as decreasing PI staining concentrations were used. This result indicates binding competition between SYBR and PI and, therefore, is in agreement with the abovementioned report (29). However, in bacteria within the R2 population, SYBR stained bright independently of the PI concentration indicating that the double positive stain (R2) was not an artefact due to fluorochromes binding competition (Fig. 2).

$SYBR^+PI^+$ represent a bacterial stage that precedes vancomycin-induced cell lysis

Several reports define the double positive bacteria as injured or in an intermediary stage between live and dead (30, 31, 32). We have thus used vancomycin, an

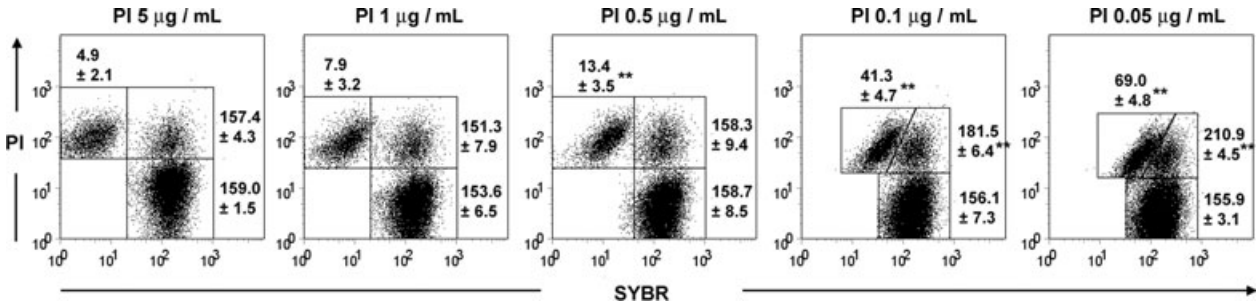

Fig. 2. Effect of PI concentration on the SYBR/PI double staining profile. Flow cytometric analysis of *S. epidermidis* cells obtained from 48-hr-grown biofilms. Cells were stained with a fixed concentration of SYBR green I (SYBR) (1:5000, commercial stock) and different concentrations of propidium iodide (PI) (5, 1, 0.5, 0.1 and 0.05 μg/mL). The numbers within dot plots correspond to the SYBR mean fluorescence intensity ± SD of bacteria gated within the defined regions ($n = 3$/group). The instrument background signal was removed from the analysis. Statistical differences between the PI 5 μg/mL staining group and all the others staining groups were analyzed with the anova Tukey's HSD post-hoc test and are indicated by asterisks ($^{**}P < 0.01$). Results are a representative example of three independent experiments.

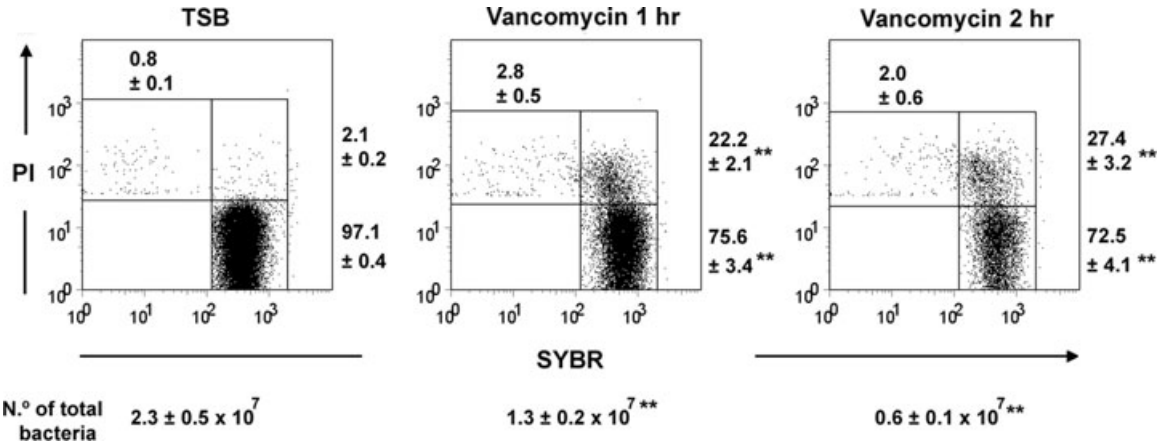

Fig. 3. Vancomycin-induced *S. epidermidis* cell lysis. Flow cytometric analysis of planktonic *S. epidermidis* cells that were allowed to grow in TSB or TSB with vancomycin (40 mg/mL) during 1 hr (Vancomycin 1 hr) or 2 hr (Vancomycin 2 hr). Cells were stained with SYBR green I (SYBR) (1:5000, commercial stock) and PI (5 μg/mL). Values within density plots correspond to the proportions ± SD of bacteria gated in the defined regions (n = 3/group). Values below the dot plots correspond to the total number of bacteria within the culture. The instrument background signal was removed from the analysis. Statistical differences between the TSB group and Vancomycin 1 hr or Vancomycin 2 hr groups were analyzed with the anova Tukey's HSD post-hoc test and are indicated by asterisks (**P<0.01). Results are a representative example of three independent experiments.

antibiotic that induces permeabilization of the cytoplasmic membrane and inhibition of cell wall synthesis in Gram-positive bacteria (33), to assess whether $SYBR^+PI^+$ bacteria (R2) could represent a physiological state that precedes cell death or lysis. As shown in Figure 3, most planktonic *S. epidermidis* 9142 bacteria obtained from an exponential phase culture were not permeable to PI (>99%). Upon a 2-hr growth in the presence of vancomycin, significant numbers of $SYBR^+PI^+$ bacteria (R2) were detected (Fig. 3). Moreover, since $SYBR^-PI^+$ bacteria (R3) did not accumulate in culture and the number of total bacteria decreased over time (Fig. 3), these results strongly suggest that double positive cells represent bacteria in a stage preceding vancomycin-induced cell lysis.

Accumulation of PI^+ bacterial cells in *S. epidermidis* biofilms over time

Glucose, as well as several other environmental factors, has been reported to induce biofilm formation *in vitro* (16,24). Others have shown that excess glucose in the culture medium led to regulated bacterial death in a process dependent of the accumulation of acidic compounds due to the metabolism of this carbon source (34). We therefore evaluated whether cell death within biofilms was associated with a glucose-dependent decrease in the culture pH. Biofilms were allowed to grow in TSB 1%G or in TSB 1%G supplemented with 100 mM hydrogen phosphate (TSB 1%G + HPO_4^{2-}). Hydrogen phosphate was used to counteract the decrease in the culture pH due to glucose metabolism (35, 36). As shown in Figure 4a, the culture pH of biofilms grown in TSB 1%G was significantly lower over time as compared to that of biofilm cultures grown in TSB 1%G + HPO_4^{2-}. Hydrogen phosphate did not impair glucose consumption (Fig. 4b) neither was it depleted from the culture medium (Fig. 4c) indicating that it acted as a buffer conferring resistance to the glucose-dependent decrease in the culture pH over time. Biofilms grown in TSB 1%G, with consequent lower culture pH, progressively accumulated higher proportions of dead bacteria ($SYBR^-PI^+$) as compared with biofilms grown in TSB 1%G + HPO_4^{2-} (Fig. 4d). This result shows an association between low culture pH and increased cell death within *S. epidermidis* biofilms. Nevertheless, biofilms grown in TSB 1%G + HPO_4^2 presented similar proportions of bacteria with the $SYBR^+PI^+$ (R2) staining profile to those detected in TSB 1%G grown biofilms (Fig. 4d). When biofilms were allowed to grow a further 24 hr (util 72 hr) in TSB 1%G or TSB 1%G + HPO_4^{2-}, a more marked difference in the accumulation of dead bacteria within biofilms was found (supplementary Fig. 2).

Evaluation of *N*-acetylglucosamine accumulation in *S. epidermidis* biofilms

PNAG is a major component of the *S. epidermidis* biofilm extracellular matrix contributing to intercellular adhesion within these bacterial communities (7). The PNAG biosynthetic precursor, *N*-acetylglucosamine, is synthesized from fructose 6-phosphate. Since abundant levels of this glycolytic intermediate are generated when bacteria were grown in medium enriched in glucose (37), we

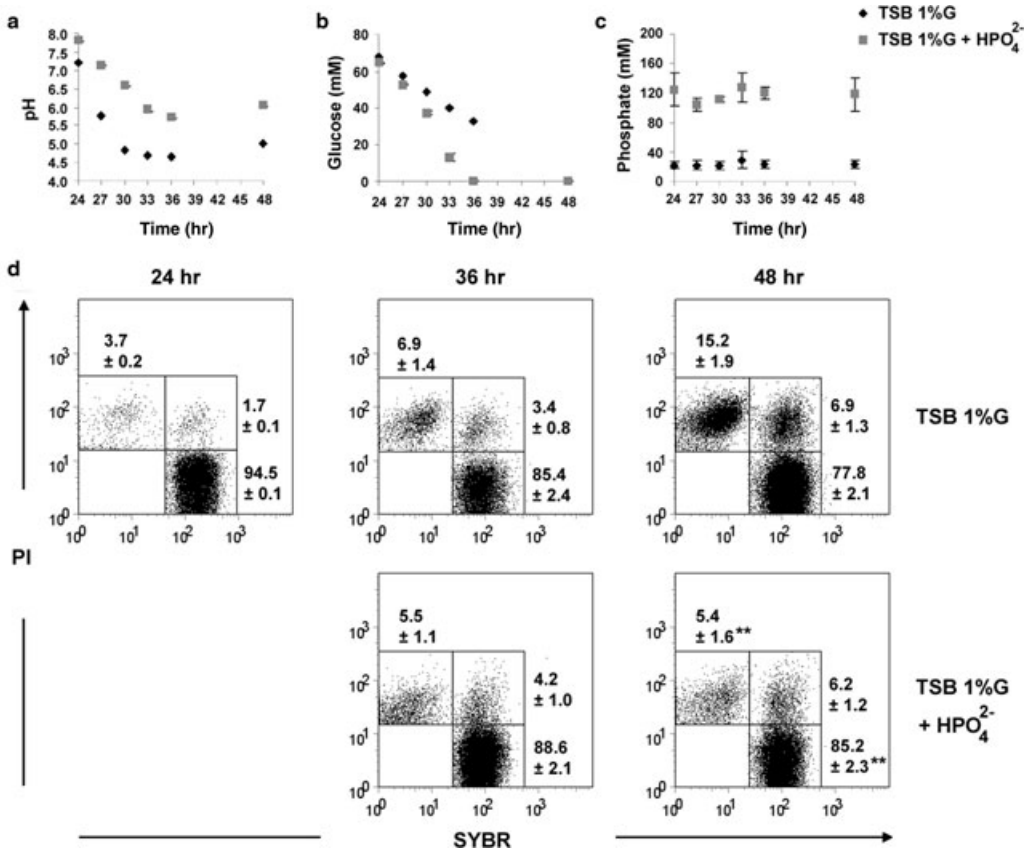

Fig. 4. Accumulation of PI^+ bacterial cells in *S. epidermidis* biofilms over time. (a) Culture pH, (b) glucose concentration and (c) phosphate concentration determined over time in the culture supernatants of established *S. epidermidis* biofilms that were allowed for an additional 24 hr growth in TSB 1%G or TSB 1%G + HPO_4^{2-}. Results are a representative example of two independent experiments ($n = 3$/group). (d) Evaluation over time (24, 36 and 48 hr) of the proportions of dead bacteria in established *S. epidermidis* biofilms that were allowed for an additional 24 hr growth in TSB 1%G or TSB 1%G + HPO_4^{2-}. Values within density plots correspond to the proportions ± SD of bacteria gated in the defined regions ($n = 3$/group). The instrument background signal was removed from the analysis. For statistical analysis, the proportions of each bacterial population (R1, R2 or R3) within biofilms grown in TSB 1%G was compared with the respective bacterial population within biofilms grown in TSB 1%G + HPO_4^{2-}. Each time point was analyzed independently. Statistical differences are indicated by asterisks (**$P < 0.01$; Student's *t*-test). Results are a representative example of three independent experiments.

evaluated PNAG accumulation in *S. epidermidis* biofilms grown in TSB 1%G or TSB 1%G + HPO_4^{2-}. Wheat germ agglutinin (WGA), a lectin that specifically binds to *N*-acetylglucosamine, was used as a probe to determine, by flow cytometry, the amount of PNAG in biofilm-grown *S. epidermidis* cells (26). As shown in Figure 5a, $SSC^{high}PI^+$ bacteria (R2) presented a higher WGA-FITC MFI than $SSC^{high}PI^-$ (R1) bacteria. This difference was more marked in biofilms grown in TSB 1%G + HPO_4^{2-} than in biofilms grown in TSB 1%G. Similar results, in respect to cell death and PNAG surface expression, were obtained when the *S. epidermidis* strains PE9, M187, JI6, IE86 and IE214 were used (supplementary Fig. 3).

We further evaluated PNAG accumulation in intact biofilms by fluorescence microscopy. In biofilms grown in TSB 1%G, PI fluorescence co-localized with WGA-FITC fluorescence indicating an association between cell death and PNAG accumulation (Fig. 5b). In biofilms grown in TSB 1%G + HPO_4^{2-}, higher amounts of PNAG, as well as a more dispersed distribution of this polymer, were observed. In these biofilms, no co-localization of PNAG with PI fluorescence was observed (Fig. 5b).

icaA expression in *S. epidermidis* biofilms

PNAG is synthesized by enzymes encoded by genes within the intercellular adhesin (*ica*) operon (*icaADBC*) (38). Since the amount and pattern of PNAG accumulation was found to differ in *S. epidermidis* biofilms grown in TSB 1%G or TSB 1%G + HPO_4^{2-}, we have evaluated bacterial *icaA* expression in these biofilms. As shown in Figure 6, an approximately 15-fold increase in *icaA* expression was

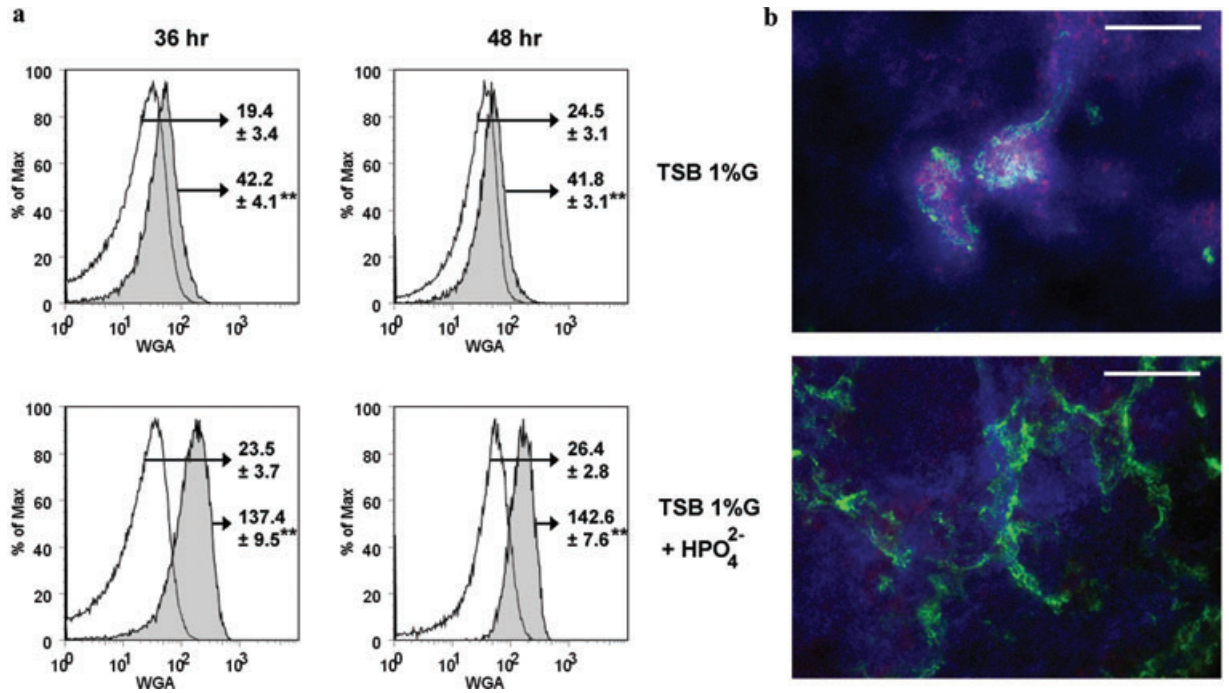

Fig. 5. PNAG accumulation in *S. epidermidis* biofilms. (a) Histogram overlay showing FITC-WGA mean fluorescence intensity (MFI) of $SSC^{high}PI^{-}$ bacteria (R1) (black histogram) and $SSC^{high}PI^{+}$ (R2) (gray-filled histogram) obtained from established *S. epidermidis* biofilms that were allowed for an additional 24 hr growth in TSB 1%G or TSB 1%G + HPO_4^{2-}. Values within histograms correspond to FITC-WGA MFI ± SD of the corresponding bacterial population ($n = 3$/group). Statistical differences are indicated by asterisks (**$P < 0.01$; Student's *t*-test). Results are a representative example of three independent experiments. (b) Evaluation of PNAG accumulation in intact *S. epidermidis* biofilms grown for 24 hr in TSB 1%G or TSB 1%G + HPO_4^{2-}. Biofilms were stained with DAPI (1 μg/mL) (blue), PI (5 μg/ml) (red) and FITC-WGA (10 μg/mL) (green). Bars correspond to 200 μm. Images are a representative example of three independent experiments.

detected in biofilms grown in TSB 1%G + HPO_4^{2-} as compared with TSB 1%G-grown biofilms. This result further suggested that culture pH influenced the accumulation of PNAG in *S. epidermidis* biofilms.

DISCUSSION

Glucose has a key role in biofilm physiology. This carbon source is generally used to promote *in vitro* the biofilm mode of growth (16,24). In the present study, the effect of glucose metabolism-dependent culture medium acidification in PNAG accumulation was evaluated. Since it was previously shown that excess glucose in *S. aureus* cultures led to regulated bacterial death due to the accumulation of acidic compounds in the culture medium (34), we first evaluated whether a similar effect would occur within *S. epidermidis* biofilms. In agreement, biofilms grown in excess glucose, which undergo progressive acidification, were found to accumulate significantly higher proportions of dead bacteria ($SYBR^{-}PI^{+}$) than biofilms grown in excess glucose with maintained pH. This indicated an association between cell death and medium acidification. Regardless of differences in cell death, both biofilms presented similar proportions of bacteria with the staining profile $SYBR^{+}PI^{+}$. These cells, despite presenting a cytoplasmic membrane permeable to PI, also presented high SSC values and bright SYBR mean fluorescence intensity indicative of high internal density and nucleic acid content. Moreover, vancomycin-induced cell lysis strongly suggested that double positive cells represented bacteria in a state preceding cell lysis. Therefore, in agreement with several other reports (30, 31, 32), $SYBR^{+}PI^{+}$ bacteria (R2) may represent an intermediary physiological state between live and dead bacteria. However, in biofilms grown in maintained pH conditions, the increase in the proportions of $SYBR^{+}PI^{+}$ bacteria was not followed by an increase in the proportions of dead cells. This opens the possibility that, in these biofilms, $SYBR^{+}PI^{+}$ bacteria may represent a particular physiological state rather than an intermediary state between live and dead. In agreement with this hypothesis, it was previously shown that PI uptake may depend on the physiological state of bacterial cells. Shi *et al.* showed that during growth in the presence of glucose, PI stained live growing cells of *Sphingomonas*

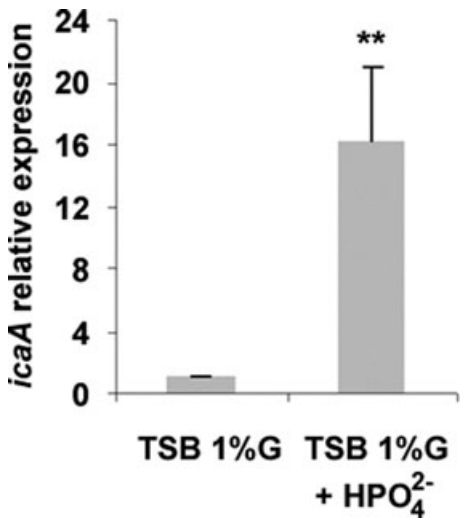

Fig. 6. *icaA* expression in *S. epidermidis* biofilms. Relative *icaA* expression in bacteria obtained from established *S. epidermidis* biofilms that were allowed to grow for an additional 9 hr in TSB 1%G or TSB 1%G + HPO_4^{2-}. Statistical differences are indicated by asterisks (**, $P < 0.01$; Student's *t*-test). Results are a representative example of three independent experiments ($n = 2$/group).

sp. and *M. frederiksbergense* during a short period of their life cycle (39).

S. epidermidis biofilms grown in excess glucose with maintained pH conditions presented higher amounts of PNAG as well as a dispersed distribution of this polymer. Single cell analysis by flow cytometry further indicated that, in these biofilms, the $SYBR^+PI^+$ subset of bacteria presented a marked increase in surface PNAG amount. This suggests differential PNAG production within biofilm bacteria, which would be in agreement with a previous report where it was proposed that bacteria within biofilms presented differential gene expression (40).

In biofilms grown in TSB 1%G, we observed that PNAG accumulation occurred in association with cell death, as assessed by co-localization of PI and WGA fluorescence. These results indicate that, depending on the *in vitro* growth conditions, different mechanisms mediate PNAG accumulation in *S. epidermidis* biofilms. Further evidence was provided by evaluation of *icaA* expression within these biofilms. Expression of this gene, encoding an enzyme responsible for PNAG synthesis, was significantly increased in biofilms grown in maintained pH conditions. Our data therefore suggests that, despite glucose abundance in both biofilm cultures, the lower culture pH found for the TSB 1%G culture medium led to decreased expression of genes encoding enzymes involved in PNAG synthesis therefore affecting the accumulation of this polymer within the biofilm matrix. A similar finding was previously reported in *S. aureus* where excess glucose, by decreasing the culture pH, led to a decreased gene expression (41).

Different clinical manifestations have been described for biofilm associated infections. Usually, the infection is not initially life threatening but subsequent exacerbations may occur often implying the surgical removal of the infected tissue or medical device (42). Since PNAG has been implicated as an important immunogenic component of the *S. epidermidis* biofilm with the ability to induce pro-inflammatory cytokine production (10), it would therefore be interesting to determine whether the biofilm PNAG content may account for its inflammatory potential and/or to the modulation of the host immune response. The herein reported *in vitro* modulation of PNAG synthesis highlights that the biofilm physiological state can be modulated by environment conditions and may be useful as a model for assessing the role of this polymer in the interaction with different components of the host immune system.

ACKNOWLEDGMENTS

The authors acknowledge the technical assistance of Encarnação Rebelo and Ângela Alves. This work was funded by Fundação para a Ciência e a Tecnologia (FCT) and COMPETE grants PTDC/BIA-MIC/113450/2009 and FCOMP-01–0124-FEDER-014309. Filipe Cerca and Ângela França were funded by FCT fellowship SFRH/BD/27638/2006 and SFRH/BD/62359/2009, respectively.

REFERENCES

1. Vuong C., Otto M. (2002) Staphylococcus epidermidis infections. *Microbes Infect* **4:** 481–9.
2. Götz F. (2002) Staphylococcus and biofilms. *Mol Microbiol* **43:** 1367–78.
3. Lewis K. (2005) Persister cells and the riddle of biofilm survival. *Biochemistry (Mosc)* **70:** 267–74.
4. Lewis K. (2007) Persister cells, dormancy and infectious disease. *Nat Rev Micro* **5:** 48–56.
5. Otto M. (2009) *Staphylococcus epidermidis* – the 'accidental' pathogen. *Nat Rev Micro* **7:** 555–67.
6. Costerton W., Veeh R., Shirtliff M., Pasmore M., Post C., Ehrlich G.. (2003) The application of biofilm science to the study and control of chronic bacterial infections. *J Clin Invest* **112:** 1466–77.
7. Mack D., Fischer W., Krokotsch A., Leopold K., Hartmann R., Egge H., Laufs R. (1996) The intercellular adhesin involved in biofilm accumulation of *Staphylococcus epidermidis* is a linear beta-1,6-linked glucosaminoglycan: purification and structural analysis. *J Bacteriol* **178:** 175–83.
8. Rupp M.E., Fey P.D., Heilmann C., Gotz F. (2001) Characterization of the importance of *Staphylococcus epidermidis* autolysin and polysaccharide intercellular adhesin in the pathogenesis of intravascular catheter associated infection in a rat model. *J Infect Dis* **183:** 1038–42.

9. Li H., Xu L., Wang J., Wen Y., Vuong C., Otto M, Gao Q. (2005) Conversion of *Staphylococcus epidermidis* strains from commensal to invasive by expression of the *ica* locus encoding production of biofilm exopolysaccharide. *Infect Immun* **73:** 3188–91.
10. Stevens N.T., Sadovskaya I., Jabbouri S., Sattar T., O'Gara J.P., Humphreys H., Greene C.M. (2009) *Staphylococcus epidermidis* polysaccharide intercellular adhesin induces IL-8 expression in human astrocytes via a mechanism involving TLR2. *Cell Microbiol* **11:** 421–32.
11. Heilmann C., Schweitzer O., Gerke C., Vanittanakom N., Mack D., Götz F. (1996) Molecular basis of intercellular adhesion in the biofilm-forming *Staphylococcus epidermidis*. *Mol Microbiol* **20:** 1083–91.
12. Cramton S.E., Ulrich M., Gotz F., Doring G. (2001) Anaerobic conditions induce expression of polysaccharide intercellular adhesin in *Staphylococcus aureus* and *Staphylococcus epidermidis*. *Infect Immun* **69:** 4079–85.
13. Knobloch J.K.-M., Bartscht K., Sabottke A., Rohde H., Feucht H.-H., Mack D. (2001) Biofilm formation by *Staphylococcus epidermidis* depends on functional RsbU, an activator of the *sigB* Operon: differential activation mechanisms due to ethanol and salt stress. *J Bacteriol* **183:** 2624–33.
14. Rachid S., Ohlsen K., Witte W., Hacker J., Ziebuhr W. (2000) Effect of subinhibitory antibiotic concentrations on polysaccharide intercellular adhesin expression in biofilm-forming *Staphylococcus epidermidis*. *Antimicrob Agents Chemother* **44:** 3357–3363.
15. Dobinsky S., Kiel K., Rohde H., Bartscht K., Knobloch J.K., Horstkotte M.A., Mack D. (2003) Glucose-related dissociation between icaADBC transcription and biofilm expression by *Staphylococcus epidermidis*: evidence for an additional factor required for polysaccharide intercellular adhesin synthesis. *J Bacteriol* **185:** 2879–86.
16. Mack D., Siemssen N., Laufs R. (1992) Parallel induction by glucose of adherence and a polysaccharide antigen specific for plastic-adherent *Staphylococcus epidermidis*: evidence for functional relation to intercellular adhesion. *Infect Immun* **60:** 2048–57.
17. Sadykov M.R., Olson M.E., Halouska S., Zhu Y., Fey P.D., Powers R., Somerville G.A. (2008) Tricarboxylic acid cycle-dependent regulation of *Staphylococcus epidermidis* polysaccharide intercellular adhesin synthesis. *J Bacteriol* **190:** 7621–32.
18. Vuong C., Kidder J.B., Jacobson E.R., Otto M., Proctor R.A., Somerville G.A. (2005) *Staphylococcus epidermidis* polysaccharide intercellular adhesin production significantly increases during tricarboxylic acid cycle stress. *J Bacteriol* **187:** 2967–2973.
19. Shu M., Wong L., Miller J.H., Sissons C.H. (2000) Development of multi-species consortia biofilms of oral bacteria as an enamel and root caries model system. *Arch Oral Biol* **45:** 27–40.
20. McNeill K., Hamilton I.R. (2003) Acid tolerance response of biofilm cells of *Streptococcus mutans*. *FEMS Microbiol Lett* **221:** 25–30.
21. Dasgupta M.K., Lam K., Ulan R.A., Bettcher K.B., Burns V., Tyrrell D.L., Dossetor J.B., Costerton J.W. (1988) An extracorporeal model of biofilm-adherent bacterial microcolony colonization for the study of peritonitis in continuous ambulatory peritoneal dialysis. *Am J Nephrol* **8:** 118–122.
22. Dasgupta M., Larabie M. (2001) Biofilms in peritoneal dialysis. *Perit Dial Int* **21:** S213–217.
23. Cerca N., Pier G., Vilanova M., Oliveira R., Azeredo J. (2004) Influence of batch or fed-batch growth on *Staphylococcus epidermidis* biofilm formation. *Lett Appl Microbiol* **39:** 420–4.
24. Yao Y., Sturdevant Daniel E., Otto M. (2005) Genomewide analysis of gene expression in *Staphylococcus epidermidis* biofilms: insights into the pathophysiology of *S. epidermidis* biofilms and the role of phenol soluble modulins in formation of biofilms. *J Infect Dis* **191:** 289–98.
25. Cerca N., Martins S., Cerca F., Jefferson K.K., Pier G.B., Oliveira R, Azeredo J. (2005) Comparative assessment of antibiotic susceptibility of coagulase-negative staphylococci in biofilm versus planktonic culture as assessed by bacterial enumeration or rapid XTT colorimetry. *J Antimicrob Chemother* **56:** 331–6.
26. Thomas V.L., Sanford B.A., Moreno R., Ramsay M.A. (1997) Enzyme-linked lectinsorbent assay measures *N*-acetyl-D-glucosamine in matrix of biofilm produced by *Staphylococcus epidermidis*. *Curr Microbiol* **35:** 249–54.
27. Cerca N., Brooks J.L., Jefferson K.K. (2008) Regulation of the intercellular adhesin locus regulator (icaR) by SarA, σB, and IcaR in *Staphylococcus aureus*. *J Bacteriol* **190:** 6530–3.
28. Rozen S., Skaletsky H. (2000) Primer3 on the WWW for general users and for biologist programmers. *Methods Mol Biol* **132:** 365–86.
29. Stocks S.M. (2004) Mechanism and use of the commercially available viability stain, BacLight. *Cytometry Part A* **61A:** 189–95.
30. Barbesti S., Citterio S., Labra M., Baroni M.D., Neri M.G., Sgorbati S. (2000) Two and three-color fluorescence flow cytometric analysis of immunoidentified viable bacteria. *Cytometry* **40:** 214–8.
31. Ben-Amor K., Heilig H., Smidt H., Vaughan E.E., Abee T., de Vos W.M. (2005) Genetic diversity of viable, injured, and dead fecal bacteria assessed by fluorescence-activated cell sorting and 16S rRNA gene analysis. *Appl Environ Microbiol* **71:** 4679–89.
32. Saegeman V.S.M., De Vos R., Tebaldi N.D., van der Wolf J.M., Bergervoet J.H.W., Verhaegen J., Lismont D., Verduyckt B., Ectors N.L. (2007) Flow cytometric viability assessment and transmission electron microscopic morphological study of bacteria in glycerol. *Microsc Microanal* **13:** 18–29.
33. Watanakunakorn C. (1984) Mode of action and in-vitro activity of vancomycin. *J Antimicrob Chemother* **14:** 7–18.
34. Rice K.C., Nelson J.B., Patton T.G., Yang S.-J., Bayles K.W. (2005) Acetic acid induces expression of the *Staphylococcus aureus cidABC* and *lrgAB* murein hydrolase regulator operons. *J Bacteriol* **187:** 813–21.
35. Manetti A.G.O., Köller T., Becherelli M., Buccato S., Kreikemeyer B., Podbielski A., Grandi G., Margarit I. (2010) Environmental acidification drives *S. pyogenes* pilus expression and microcolony formation on epithelial cells in a FCT-dependent manner. *PLoS ONE* **5:** e13864.
36. Goodwin S., Zeikus J.G. (1987) Physiological adaptations of anaerobic bacteria to low pH: metabolic control of proton motive force in *Sarcina ventriculi*. *J Bacteriol* **169:** 2150–7.
37. Sadykov M.R., Mattes T.A., Luong T.T., Zhu Y., Day S.R., Sifri C.D., Lee C.Y., Somerville G.A. (2010) Tricarboxylic acid cycle-dependent synthesis of *Staphylococcus aureus* type 5 and 8 capsular polysaccharides. *J Bacteriol* **192:** 1459–62.
38. Cramton S.E., Gerke C., Schnell N.F., Nichols W.W., Gotz F. (1999) The intercellular adhesion (*ica*) locus is present in *Staphylococcus aureus* and is required for biofilm formation. *Infect Immun* **67:** 5427–33.
39. Shi L., Günther S., Hübschmann T., Wick L.Y., Harms H., Müller S. (2007) Limits of propidium iodide as a cell viability indicator for environmental bacteria. *Cytometry Part A* **71A:** 592–8.
40. Beenken K.E., Dunman P.M., McAleese F., Macapagal D., Murphy E., Projan S.J., Blevins J.S., Smeltzer M.S. (2004) Global gene expression in *Staphylococcus aureus* biofilms. *J Bacteriol* **186:** 4665–84.
41. Regassa L.B., Novick R.P., Betley M.J. (1992) Glucose and nonmaintained pH decrease expression of the accessory gene regulator (*agr*) in *Staphylococcus aureus*. *Infect Immun* **60:** 3381–88.

42. Wolcott R.D., Ehrlich G.D. (2008) Biofilms and chronic infections. *JAMA* **299:** 2682–4.

SUPPORTING INFORMATION

Additional supporting information may be found in the online version of this article:

Fig. S1. (A) *S. epidermidis* bacteria obtained from an exponential-phase planktonic culture, presenting less than 0.1% of PI^+ cells, were sonicated as above described during 10 cycles of 10 s. Damage in the cytoplasmic membrane was assessed by PI incorporation at sonication cycles 1, 5 and 10. Viable cell concentration and culturability were determined by flow cytometry and spread plating, respectively. These results show that sonication does not affect the bacterial cytoplasmic membrane integrity as no increase in PI^+ cells was detected. This treatment also did not affect cell culturability or induce cell lysis as the concentration of viable and culturable cells maintained constant over the sonication cycles. (B) The effect of sonication on the disaggregation of bacterial clumps was also evaluated. *S. epidermidis* bacteria obtained from biofilms grown in TSB 1%G + HPO_4^{2-} were sonicated as described above and bacterial aggregates were analyzed by flow cytometry assessing Forward (size) and Side (internal complexity) scatter profiles of the cell samples before and after treatment. It is shown that after sonication bacterial aggregates, defined as $FSC^{high}SSC^{high}$, were reduced to less than 0.1%, a value similar to that detected in free-floating planktonic cultures. Moreover, cell aggregation was found to occur mainly in the $SYBR^+PI^+$ bacterial population as determined by an increased SYBR and PI fluorescence detected in these bacteria before sonication.

Fig. S2. Established 48 hr biofilms, grown in TSB 1%G or TSB 1%G + HPO_4^{2-} as described were allowed to grow for an additional 24 hr in TSB 1%G or TSB 1%G + HPO_4^{2-}. These 72 hr biofilms were then evaluated in respect to cell death. The instrument background signal was removed from the analysis. Values within density plots correspond to the proportions ± SD of bacteria gated in the defined regions. Statistical differences are indicated by asterisks (**, $P < 0.01$; Student's *t*-test). Results are a representative example of three independent experiments ($n = 3$/group).

Fig. S3. (A) Evaluation of cell death in established *S. epidermidis* biofilms that were allowed for an additional 24 hr growth in TSB 1%G or TSB 1%G + HPO_4^{2-}. The *S. epidermidis* strains PE9, M187, JI6, IE86 and IE214 were used. Values within density plots correspond to the proportions ± SD of bacteria gated in the defined regions ($n = 2$/group). The instrument background signal was removed from the analysis. For statistical analysis, the proportions of each bacterial population (R1, R2 or R3) within biofilms grown in TSB 1%G was compared with the respective bacterial population within biofilms grown in TSB 1%G + HPO_4^{2-}. Statistical differences are indicated by asterisks (**, $P < 0.01$; Student's *t*-test). Results are a representative example of two independent experiments. For all strains, the proportions of dead bacteria ($SYBR^-PI^+$) within biofilms grown in TSB 1%G were significantly higher as compared with biofilms grown in TSB 1%G + HPO_4^{2-}. (B) Histogram overlay showing FITC-WGA mean fluorescence intensity (MFI) of $SSC^{high}PI^+$ bacteria (R2) obtained from biofilms grown in TSB 1%G (black histogram) and $SSC^{high}PI^+$ bacteria (R2) obtained from biofilms grown in TSB 1%G + HPO_4^{2-} (gray-filled histogram). Values within histograms correspond to FITC-WGA MFI ± SD of the corresponding bacterial population ($n = 2$/group). Statistical differences are indicated by asterisks (**, $P < 0.01$; Student's *t*-test). Results are a representative example of two independent experiments. For all strains, the amount of surface PNAG in PI-incorporating bacteria was significantly higher in bacteria obtained from biofilms grown in TSB 1%G + HPO_4^{2-} than in bacteria obtained from biofilms grown in TSB 1%G.

Please note: Wiley–Blackwell are not responsible for the content or functionality of any supporting materials supplied by the authors. Any queries (other than missing material) should be directed to the corresponding author for the article.